Journal of Power Sources 199 (2012) 426–431

Contents lists available at SciVerse ScienceDirect

Journal of Power Sources

journal homepage: www.elsevier.com/locate/jpowsour

Triphenylamine-based starburst dyes with carbazole and phenothiazine antennas for dye-sensitized solar cells

ZhongQuan Wan [a], ChunYang Jia [a,*], JiaQiang Zhang [a], YanDong Duan [b], Yuan Lin [b,**], Yu Shi [a]

[a] State Key Laboratory of Electronic Thin Films and Integrated Devices, School of Microelectronics and Solid-State Electronics, University of Electronic Science and Technology of China, Chengdu 610054, PR China
[b] CAS Key Laboratory of Photochemistry, Institute of Chemistry, BNLMS, Chinese Academy of Sciences, Beijing 100190, PR China

ARTICLE INFO

Article history:
Received 1 May 2011
Received in revised form 31 August 2011
Accepted 17 October 2011
Available online 20 October 2011

Keywords:
Triphenylamine
Starburst
Carbazole
Phenothiazine
Dye-sensitized solar cells
Rhodanine-3-acetic acid

ABSTRACT

Two new triphenylamine-based starburst dyes (**WD-2** and **WD-3**) are designed, in which the carbazole/phenothiazine groups are used as secondary electron donor and the rhodanine-3-acetic acid moiety as the acceptor. We report the synthesis, photophysical and electrochemical properties of the dyes as well as their applications in dye-sensitized solar cells (DSSCs). Under standard global AM 1.5 solar condition, the **WD-2** sensitized cell gives a short circuit photocurrent density J_{sc} = 6.4 mA cm^{-2}, an open circuit voltage V_{oc} = 600 mV, a fill factor ff = 0.8, corresponding to an overall conversion efficiency of 3.1%. Under the same conditions, the **WD-3** sensitized cell gives J_{sc} = 4.7 mA cm^{-2}, V_{oc} = 570 mV, and ff = 0.78, corresponding to an overall conversion efficiency of 2.1%. The conversion efficiency is increased about 47% from **WD-2** sensitized cell to **WD-3** sensitized cell. The research results show that the inefficient electron injection from the excited dyes into the conduction band of TiO_2 results in the low efficiencies of DSSCs based on the two dyes.

1. Introduction

As petroleum and coal are depleted, renewable energy sources have been attracted increasing attention in recent years, and solar energy is considered as a good alternate for fossil fuel energy. In comparison with the traditional silicon-based solar cells [1], dye-sensitized solar cells (DSSCs) is one of the most promising next-generation photovoltaic cells due to its simple, cheap, and environmental friendly. Therefore, DSSCs has been attracted much attention since the breakthrough made by Grätzel and co-workers [2]. In DSSCs, dye sensitizer is one of the key components for high conversion efficiencies. The most successful sensitizers employed so far in DSSCs are several ruthenium-based sensitizers, such as **N3** [3], **N719** [4], and black dye [5], which have achieved remarkable conversion efficiencies of 10–11%.

In spite of this, the main drawbacks of the ruthenium based sensitizers are the lack of absorption in the red region of the solar spectrum as well as rarity of the metal in the earth crust. Consequently, many researchers have focused on developing metal-free organic sensitizers [6–15], which possess some advantages over ruthenium-based sensitizers: ease of synthesis, high molar extinction coefficient, tunable absorption spectral response from the visible to the near infrared (NIR) region, as well as environmentally friendly and inexpensive production techniques. Many novel organic sensitizers such as coumarin [6], merocyanine [7], indoline [8], polyene [9], hemicyanine [10], triphenylamine [11], fluorene [12], carbazole [13], tetrahydroquinoline [14] and phenothiazine [15] based organic dyes have been developed and showed good performances.

Most organic dyes contain a structure of donor–π linker–acceptor (D–π–A). The dyes with this structure usually have a rod-like configuration. However, the rod-like molecules are elongated, which may facilitate the recombination of electrons with the triiodide and the formation of aggregations between molecules [16]. The close π–π aggregation can not only lead to self-quenching and reduction of electron injection into TiO_2, but also bring to the instability of the organic dyes due to the formation of excited triplet states and unstable radicals under light irradiation [17]. Therefore, the dyes with a starburst conformation are designed and synthesized by introducing starburst donor units into the D–π–A molecule to form the D–D–π–A structure [18], which has the following merits: (1) avoids the charge recombination processes of injected electrons with triiodide in the electrolyte. (2) the absorption region can be extended and the molar extinction coefficient can be enhanced. (3) lower tendency to aggregate and better thermo-stability. The great performance of organic dyes with D–D–π–A structure over the simple D–π–A configuration can be achieved by molecular design [8b,18b].

* Corresponding author. Tel.: +86 28 83202550; fax: +86 28 83202569.
** Corresponding author. Tel.: +86 10 82615031; fax: +86 10 82617315.
E-mail addresses: cyjia@uestc.edu.cn (C. Jia), linyuan@iccas.ac.cn (Y. Lin).

0378-7753/$ – see front matter © 2011 Elsevier B.V. All rights reserved.
doi:10.1016/j.jpowsour.2011.10.062

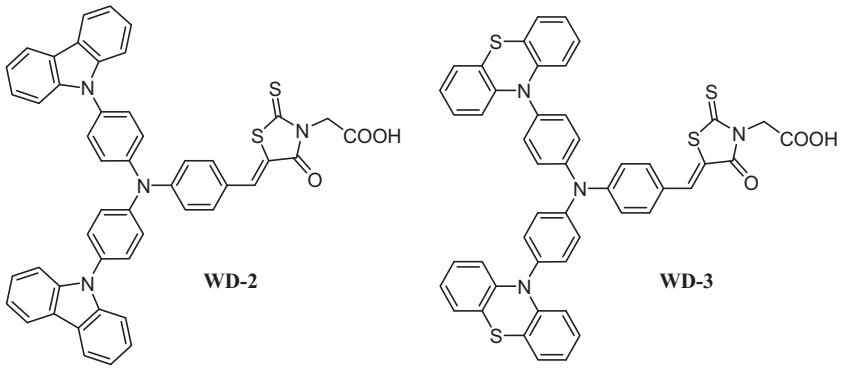

Scheme 1. Molecular structures of **WD-2** and **WD-3**.

In this study, we design and synthesize two new starburst triarylamine based organic sensitizers (**WD-2** and **WD-3**) with D–D–π–A structure by adding electron donor groups (carbazole and phenothiazine) on the outside of triarylamine, and rhodanine-3-acetic acid as the electron acceptor (Scheme 1). The photophysical/electrochemical properties of the dyes and the photovoltaic performances of the DSSCs based on the dyes are studied.

2. Results and discussion

2.1. UV–vis absorption/emission spectra

In the dye-sensitized solar cells, photosensitizer is a pivotal and unique component with a function of light-harvesting. Its spectral response overlaping with the solar spectrum has great influence on the device photocurrent. Therefore, we first measure the absorption spectra of the two dyes to have a preliminary evaluation on their light-harvesting capacities.

The UV–vis absorption spectra of the two dyes in CH_2Cl_2 are shown in Fig. 1. The two dyes exhibit one visible absorption band, appearing at 400–520 nm, which can be ascribed to an efficient charge-separated state produced by an intramolecular charge transfer (ICT) between the donor and the rhodanine-3-acetic acid. The absorption spectra of **WD-2** has one intense visible absorption band centered at 473 nm (λ_{max}) with molar extinction coefficient (ε) of 43 000 M^{-1} cm^{-1}. On the other hand, **WD-3** exhibits an absorption λ_{max} at 468 nm with a molar extinction coefficient of 25 250 M^{-1} cm^{-1}. This value is much lower than that of **WD-2**, which maybe due to the introduction of phenothiazine unit brings the decrease of co-planarity between the electron donor and the electron acceptor in the ground-state [19]. In comparison with **WD-3**, the molar extinction coefficient of **WD-2** is higher, which is an advantageous spectral property for harvesting the light.

Furthermore, the emission spectra of **WD-2** and **WD-3** are measured in CH_2Cl_2 and the corresponding maximum emission located at 599 and 543 nm, respectively (Fig. 2). Based on the intersection of absorption and emission spectra, the zeroth–zeroth transition energies (E_{0-0}) of **WD-2** and **WD-3** are estimated to be 2.354 and 2.476 eV, respectively.

2.2. Electrochemical properties

The energetic alignment of the HOMO and LUMO energy levels is crucial for the efficient operation of a sensitizer in DSSCs. To ensure efficient electron injection from the excited dye into the conduction band of TiO_2, the LUMO level must be higher than the TiO_2 conduction band edge. The HOMO level of the dye must be lower than the redox potential of the I^-/I_3^- redox couple for efficient regeneration of the dye cation after photoinduced electron injection into the TiO_2 film. To judge the possibility of electron transfer from the excited dye to the conductive band of TiO_2, cyclic voltammetry is performed to determine redox potentials of the two dyes.

As shown in Fig. 3 and Table 1, the first oxidation potentials (E_{ox}) of the dyes (**WD-2**: 0.457 V vs NHE; **WD-3**: 0.410 V vs NHE) are more positive than the I^-/I_3^- redox potential (0.4 V vs NHE), which indicates that the oxidized dyes favorably accept electrons from I^- ions in thermodynamic property. This can lead to dye-regeneration, avoiding the charge recombination between oxidized dyes and photoinjected electrons in the nanocrystalline TiO_2 film. On the other hand, the excited-state oxidation potentials (E^*_{ox}) of the dyes are calculated from the first oxidation potentials and the E_{0-0}, which is determined from the intersection of absorption and

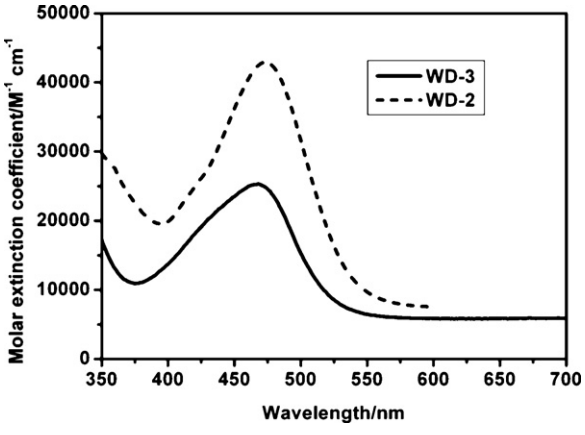

Fig. 1. Absorption spectra of **WD-2** and **WD-3** in CH_2Cl_2.

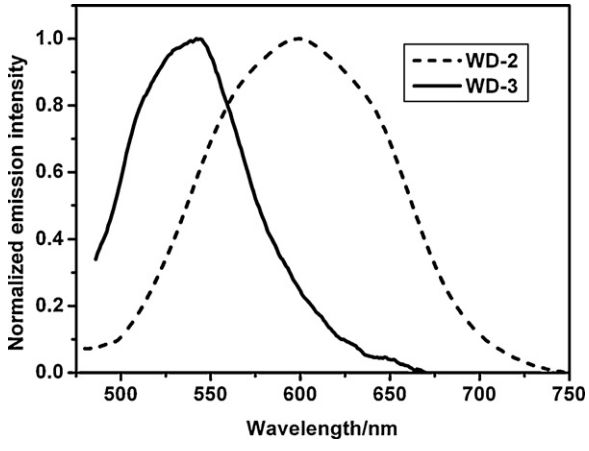

Fig. 2. Emission spectra of **WD-2** and **WD-3** in CH_2Cl_2.

Table 1
UV–vis, emission and electrochemical data.

Dye	λ_{max}[a]/nm (ε[b]/M^{-1} cm^{-1})	λ_{ex}[a]/nm	E_{ox}[c]/V (vs NHE)	E_{0-0}[d]/eV	E^*_{ox}[e]/V (vs NHE)
WD-2	473 (43 000)	599	0.457	2.354	−1.897
WD-3	468 (25 250)	543	0.410	2.476	−2.066

[a] Absorption and emission spectra were measured in CH_2Cl_2 (2.5×10^{-5} M) at room temperature.
[b] The molar extinction coefficient at λ_{max} of the absorption spectra.
[c] The first oxidation potential of the dye was measured in DMF with 0.1 M n-Bu_4NPF_6 as electrolyte (scanning rate: 100 mV s^{-1}, Pt wires as working electrode and counter electrode, and Ag/AgCl as reference electrode), potentials measured vs Ag/AgCl were converted to normal hydrogen electrode (NHE) by addition of +0.2 V.
[d] 0–0 transition energy, estimated from the intersection between the absorption and emission spectra in CH_2Cl_2.
[e] The E^*_{ox} of the dyes were calculated from $E_{ox} - E_{0-0}$.

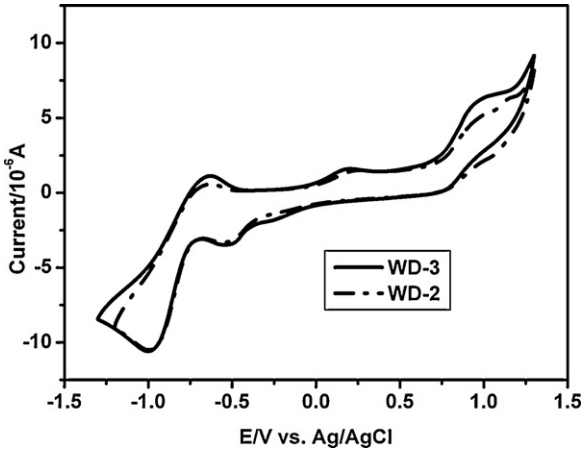

Fig. 3. Cyclic voltammograms of **WD-2** and **WD-3** in DMF.

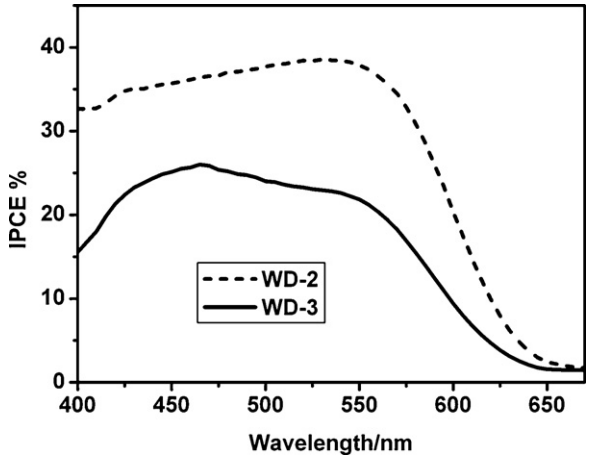

Fig. 5. The IPCE spectra of the DSSCs sensitized with **WD-2** and **WD-3**.

emission spectra. The excited state oxidation potentials (E^*_{ox}) of the dyes (**WD-2**: −1.897 V vs NHE; **WD-3**: −2.066 V vs NHE) are far more negative than the band edge energy of the nanocrystalline TiO_2 electrode (−0.5 V vs NHE) [20], indicating that the electron injection process from the excited dye molecule to TiO_2 conduction band is energetically permitted. Therefore, the two dyes can have sufficient driving force for electron transfer from the excited dye molecule to the conduction band of TiO_2 electrode. These results clearly demonstrate that the dyes are potentially efficient sensitizers for DSSCs. The schematic energy levels of **WD-2** and **WD-3** based on absorption and electrochemical data are shown in Fig. 4.

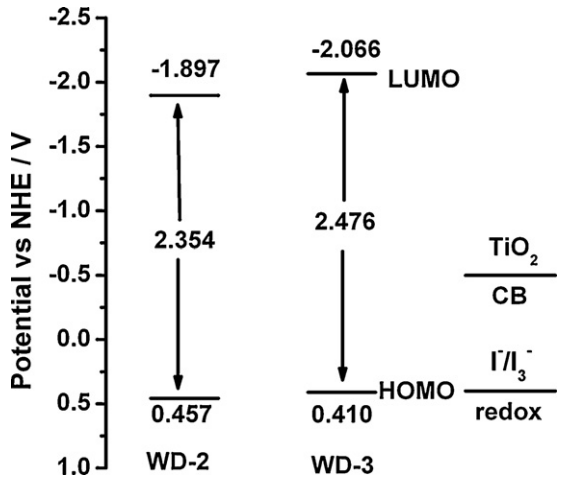

Fig. 4. Schematic energy levels of **WD-2** and **WD-3** based on absorption and electrochemical data.

2.3. Photovoltaic properties

The incident photon-to-current conversion efficiencies (IPCE) of the DSSCs based on **WD-2** and **WD-3** are measured in the visible region (400–800 nm), as shown in Fig. 5. It can be seen that the photocurrent response of **WD-2** sensitized DSSCs is better, and its maximum IPCE (39%) is obtained at 532 nm. The IPCE of **WD-3** is much lower than that of **WD-2**, and its maximum IPCE (26%) is obtained at 465 nm. In comparison with **WD-3**, **WD-2** gives the higher IPCE value, which shows a relatively large photocurrent in the corresponding DSSCs. The higher IPCE value of **WD-2** maybe due to the higher molar extinction coefficient. On the other hand, the IPCE values for **WD-2** and **WD-3** obviously decrease after 550 nm, which can be attributed to the decrease of light harvesting properties.

Fig. 6 shows the J–V curves of the DSSCs based on **WD-2** and **WD-3** dyes. The photovoltaic data are summarized in Table 2. Similar as the result of IPCE, the photovoltaic data show the order of **WD-3** < **WD-2**. For the DSSCs based on **WD-2**, an overall conversion efficiency of 3.1% is obtained with J_{sc} = 6.4 mA cm^{-2}, V_{oc} = 600 mV, and ff = 0.8. Under the same conditions, the **WD-3** sensitized cell gives J_{sc} = 4.7 mA cm^{-2}, V_{oc} = 570 mV, and ff = 0.78, and an overall conversion efficiency of 2.1%. An increase in η of about 47% is obtained from **WD-3** to **WD-2**. The values of the DSSCs based

Table 2
Photovoltaic performances of the DSSCs sensitized with **WD-2**, **WD-3** and **N3**.[a]

Dye	J_{sc}/mA cm^{-2}	V_{oc}/mV	ff	η/%
WD-2	6.4	600	0.80	3.1
WD-3	4.7	570	0.78	2.1
N3	17.2	650	0.71	7.9

[a] Photovoltaic performances of the DSSCs sensitized with **WD-2**, **WD-3** and **N3** were obtained without any coadsorption addition such as chenodeoxycholic acid, which is usually applied for preventing dye aggregation.

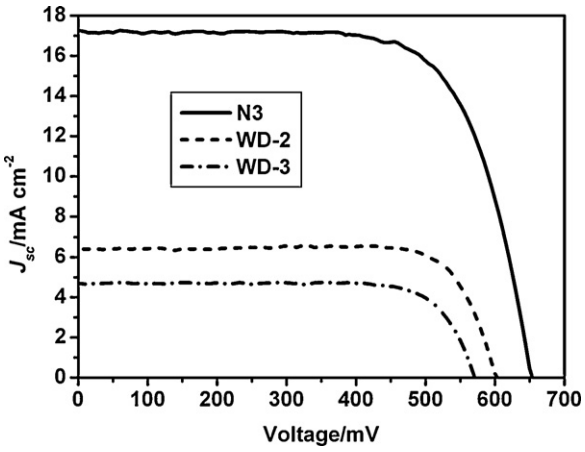

Fig. 6. Current density–voltage curves of the DSSCs sensitized with **WD-2** and **WD-3**.

on **N3** (J_{sc} = 17.2 mA cm^{-2}, V_{oc} = 650 mV, ff = 0.71, and η = 7.9%) are obtained under the same conditions.

According to Fig. 6 and Table 2, it is clear that the photovoltaic performances of the DSSCs can be evidently affected by carbazole/phenothiazine moieties in the dye molecules. In comparison with **WD-3**, the J_{sc} and V_{oc} values of **WD-2** are significantly improved by introducing carbazole moieties as the secondary donor. The broader and higher IPCE of **WD-2** likely results in a higher J_{sc} value compared with that of **WD-3**. The V_{oc} of **WD-2** is higher than that of **WD-3** might be due to the comparatively lower HOMO (E_{ox}) (estimated from the CV), which offers larger driving force for the reduction of the oxidized dye. This, in turn, leads to a slower back electron transfer from TiO_2 to the oxidized dye and result in a lager V_{oc} value [19]. The higher J_{sc} and V_{oc} for the corresponding DSSCs based on **WD-2** lead to the higher efficiency (3.1%) finally.

2.4. Theoretical calculations

To gain insight into the geometrical and electronic properties of the two dyes, their geometries are optimized by density functional theory (DFT) calculations at the B3LYP/6-31G(d,p) level with Gaussian 03 program [21]. All dihedral angles between carbazole/phenothiazine and benzene are all noncoplanar, which can help to inhibit the close π–π aggregation effectively between the starburst structures. The noncoplanar configuration can also reduce contact between molecules and enhance their thermo-stability [22]. Fig. 7 shows the electron distribution of the HOMO and LUMO of **WD-2** and **WD-3**. At the ground state (HOMO) for the two dyes, electrons are mainly distributed on the electron donor groups. However, at the excited state (LUMO), the intramolecular charge transfer leads to the electron movement from the donor group to the rhodanine ring. For the LUMO orbitals of the two dyes, which are mainly concentrated on the rhodanine framework, especially on the carbonyl and thiocarbonyl. Due to the presence of the –CH_2– group, the position of LUMO isolated from the –COOH anchoring group. Consequently, the dyes cannot give fast electron injection from the their LUMO orbitals to TiO_2 conduction band [23], so the dyes with the good absorption characteristics show the low solar cell efficiency.

3. Conclusions

In summary, two new triphenylamine-based starburst dyes (**WD-2** and **WD-3**) with carbazole/phenothiazine antennas are designed and synthesized. The photophysical and electrochemical

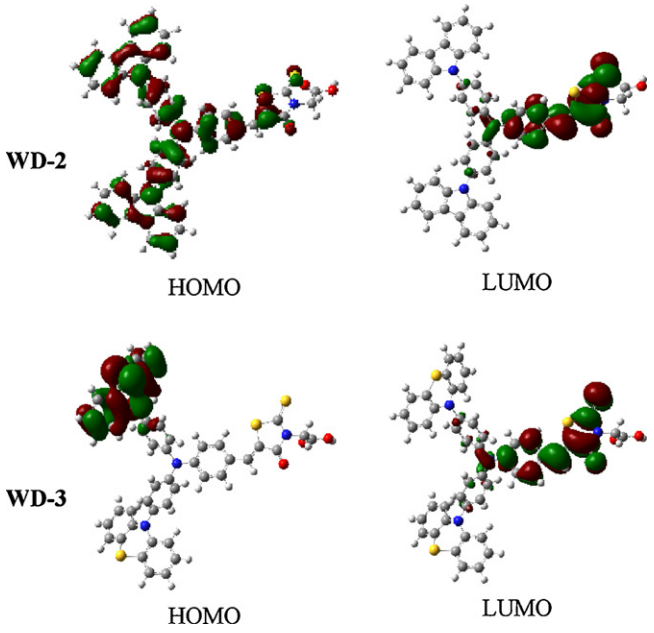

Fig. 7. The frontier orbitals of **WD-2** and **WD-3** optimized at the B3LYP/6-31+G(d,p) level.

properties of the two dyes are studied. From the first oxidation potentials and the excited-state oxidation potentials of the dyes, it is clear that the excited electrons can be injected into the TiO_2 conduction band and the oxidized dyes can be reduced by taking electrons from redox electrolyte. Under standard global AM 1.5 solar condition, the DSSCs based on **WD-2** show an overall conversion efficiency of 3.1%, comparing to 2.1% for the DSSCs based on **WD-3** under the same experimental conditions. The conversion efficiency is increased about 47% from the **WD-3** sensitized DSSCs to **WD-2** sensitized DSSCs, which can be ascribed to the higher IPCE and lower HOMO of **WD-2**. The dyes have the good absorption characteristics, but the DSSCs based on these two dyes show the low efficiencies, which maybe due to inefficient electron injection from the excited dyes (rhodanine-3-acetic acid as the electron acceptor) into the conduction band of TiO_2. Further modifications on electron acceptor and π-conjugation system of these two dyes which may improve the solar cell performance are in progress and will be published soon.

4. Experimental details

4.1. Materials and characterization

The synthetic routes of the two dyes are shown in Scheme 2. All solvents and other chemicals are reagent grade and used without further purification. 3-hexyl-1-methylimidazolium Iodide (HMII) was prepared according to the literature [24]. Lithium iodide (LiI) was purchased from Acros. Rhodanine-3-acetic acid, 4-tert-butylpyridine (TBP) and 3-methoxypropionitrile (MPN) were purchased from Aldrich. Phenothiazine, carbazole and triphenylamine were purchased from Astatech. The melting points were taken on X-4 melting point apparatus. ^{1}H and ^{13}C NMR spectra were recorded on Bruker 400 and 600 MHz spectrometers, respectively. TOF-MS spectra were determined with a BEFLEX III spectrometer. HRMS data were determined with an FTICR-APEX instrument.

4.2. Photophysical and electrochemical measurements

Absorption spectra were measured with SHIMADZU (model UV1700) UV–vis spectrophotometer. Emission spectra were

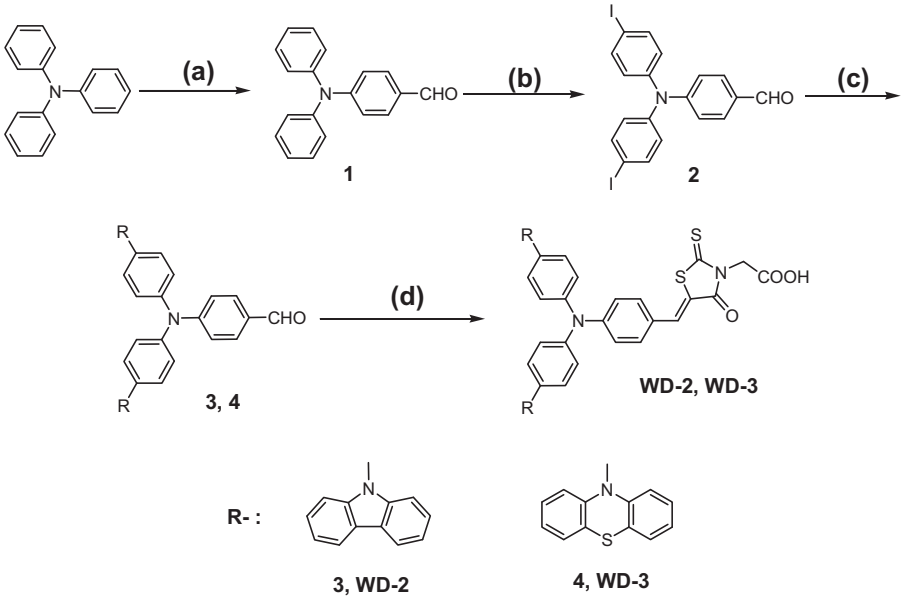

Scheme 2. Synthetic route of **WD-2** and **WD-3**. (a) $POCl_3$, DMF, 1,2-dichloroethane, reflux, 12 h; (b) KI, KIO_3, CH_3COOH, 80 °C, 4 h; (c) phenothiazine or carbazole, 1,2-dichlorobenzene, Cu, K_2CO_3, 18-crown-6, reflux, 48 h; (d) rhodanine-3-acetic acid, CH_3CN/piperidine, reflux, 15 h.

recorded with Hitachi (model RF-5301) spectrophotometer. Cyclic voltammetry experiments were performed on CH Instruments 660C electrochemical workstation with scan rate of 100 mV s^{-1} in dimethylformamide (DMF) (5.0×10^{-4} M) containing 0.1 M *n*-Bu_4NPF_6 as the supporting electrolyte, platinum as counter and work electrodes and Ag/AgCl as reference electrode.

4.3. Fabrication of DSSCs

TiO_2 colloid was prepared according to the literature [25]. The FTO glass substrates were immersed in 40 mM $TiCl_4$ aq. at 70 °C for 30 min and washed with water and ethanol. The 12 μm thick mesoporous nano-TiO_2 films composed of 15–20 nm anatase TiO_2 particles were coated on the FTO glass plates by doctor blade. After drying the nanocrystalline TiO_2 layer at 125 °C, a 4 μm light scattering layer with 300–500 nm anatase particles (Shanghai Cai Yu Nano Technology Co., Ltd., http://shkangyu.cn.gongchang.com) was deposited by doctor blade onto the first layer. The TiO_2 electrodes were heated at 450 °C for 30 min. After the sintering, when the temperature cooled to about 90 °C, the electrodes were immersed in a dye bath containing 0.5 mM **N3** in ethanol or 0.2 mM **WD-2** and **WD-3** in acetonitrile and kept overnight. The films were then rinsed in ethanol to remove excess dye. Solar cells were assembled, using a 25 μm thick thermoplastic Surlyn frame and a platinized counter electrode. An electrolyte solution was then introduced through the hole predrilled in the counter electrode, and the cell was sealed with thermoplastic Surlyn film and a glass coverslip. The electrolyte employed was a solution of 0.3 M HMII, 0.5 M LiI, 0.05 M I_2 and 0.5 M TBP in MPN.

4.4. Characterization of DSSCs

The irradiation source for the photocurrent density–voltage (*J*–*V*) measurement is an AM 1.5 solar simulator (91160A, Newport Co., USA). The incident light intensity was 100 mW cm^{-2} calibrated with a standard Si solar cell. The tested solar cells were masked with a working area of 0.2 cm^2. Volt–current characteristic were performed on a Model 2611 source meter (Keithley Instruments, Inc., USA). A Keithley 2611 source meter and a Model spectrapro 300i monochromator (Acton research, USA) equipped with a 500 W xenon lamp (Aosiyuan Technology & Science Co., Ltd., China) were used for IPCE measurements.

4.5. Computational methods

Gaussian 03 package was used for density functional theory (DFT) calculations [21]. We optimized the geometries of **WD-2** and **WD-3** using the B3LYP method with the 6-31G(d,p) basis set. Importantly, none of the frequency calculations generated negative frequencies, being consistent with an energy minimum for the optimized geometry.

4.6. Preparation of *WD-2* and *WD-3*

The synthetic routes of **WD-2** and **WD-3** are shown in Scheme 2. Compound **1** [26], **2** [27], **3** [27] and **4** [27] were prepared according to the reported procedures.

4.6.1. (Z)-2-(5-(4-(bis(4-(9H-carbazol-9-yl)phenyl)amino)benzylidene)-4-oxo-2-thioxothiazolidin-3-yl)acetic acid (*WD-2*)

A CH_3CN (10 mL) solution of compound **3** (120 mg, 0.2 mmol), rhodanine-3-acetic acid (57 mg, 0.3 mmol) and a few drops of piperidine was charged sequentially in a three-necked flask and heated to reflux for 15 h. After cooling to room temperature, solvents were removed by rotary evaporation, and the residue was purified by silica gel column chromatography with CH_2Cl_2:CH_3OH (10:1, v:v) as eluent to afford **WD-2** as a dark red solid (100 mg, yield 64%). mp 276–278 °C. ^1H NMR (400 MHz, DMSO-d_6): δ 8.27 (d, *J* = 7.6 Hz, 4H), 7.87 (s, 1H), 7.71 (t, 6H), 7.58 (d, *J* = 8.4 Hz, 4H), 7.47 (t, 8H), 7.31 (t, 6H), 4.75 (s, 2H). ^{13}C NMR (150 MHz, DMSO-d_6): 194.2, 168.6, 167.8, 151.1, 145.8, 141.4, 135.1, 134.8, 134.3, 129.6, 128.6, 127.5, 127.0, 124.0, 122.1, 121.8, 121.4, 119.3, 111.0, 46.3. MALDI-TOF (*m*/*z*): calcd for $C_{48}H_{32}N_4O_3S_2$: 776.2, found 776.5 $[M]^+$. HRMS-EI (*m*/*z*): calcd for $C_{48}H_{32}N_4O_3S_2$, 776.1916; found, 776.1890.

*4.6.2. (Z)-2-(5-(4-(bis(4-(10H-phenothiazin-10-yl)phenyl)amino)benzylidene)-4-oxo-2-thioxothiazolidin-3-yl)acetic acid (**WD-3**)*

A synthetic procedure similar as that for preparing dye **WD-2** but with compound **4** instead of compound **3**. The dye **WD-3** is dark red solid (yield 60%), mp 225–227 °C. ^{1}H NMR (400 MHz, DMSO-d_6): δ 7.73 (s, 1H), 7.62 (d, J = 7.8 Hz, 2H), 7.46–7.40 (m, 8H), 7.27 (d, J = 8.2 Hz, 2H), 7.10 (d, 4H), 7.01 (t, 4H), 6.90 (t, 4H), 6.40 (d, J = 8.0 Hz, 4H), 4.37 (s, 2H). ^{13}C NMR (150 MHz, DMSO-d_6): 194.1, 168.3, 157.4, 150.3, 146.4, 144.8, 138.0, 133.9, 133.2, 132.5, 128.7, 128.6, 128.0, 124.2, 123.2, 121.2, 121.0, 119.5, 118.0, 48.2. MALDI-TOF (m/z): calcd for $C_{48}H_{32}N_4O_3S_4$: 840.1, found 840.1 $[M]^+$. HRMS-EI (m/z): calcd for $C_{48}H_{32}N_4O_3S_4$, 840.1357; found, 840.1346.

Acknowledgments

We thank the National Natural Science Foundation of China (Grant Nos. 20602005, 20873015), the Fundamental Research Funds for the Central Universities (Grant No. E022050205) and the Innovation Funds of State key Laboratory of Electronic Thin Films and Integrated Device (Grant No. CXJJ201104) for financial support.

References

[1] A. Goetzberger, C. Hebling, H.W. Schock, Mater. Sci. Eng. R 40 (2003) 1.
[2] (a) B. O'Regan, M. Grätzel, Nature 353 (1991) 737;
(b) M. Grätzel, Nature 414 (2001) 338.
[3] M. Grätzel, J. Photochem. Photobiol. A 168 (2004) 235.
[4] M.K. Nazeeruddin, A. Kay, L. Rodicio, R. Humphry-Baker, E. Müller, P. Liska, N. Vlachopoulos, M. Grätzel, J. Am. Chem. Soc. 115 (1993) 6382.
[5] M.K. Nazeeruddin, P. Péchy, T. Renouard, S.M. Zakeeruddin, R. Humphry-Baker, P. Comte, P. Liska, L. Cevey, E. Costa, V. Shklover, L. Spiccia, G.B. Deacon, C.A. Bignozzi, M. Grätzel, J. Am. Chem. Soc. 123 (2001) 1613.
[6] (a) K. Hara, K. Sayama, Y. Ohga, A. Shinpo, S. Suga, H. Arakawa, Chem. Commun. (2001) 569;
(b) K. Hara, Z.S. Wang, T. Sato, A. Furube, R. Katoh, H. Sugihara, Y. Dan-oh, C. Kasada, A. Shinpo, S. Suga, J. Phys. Chem. B 109 (2005) 15476;
(c) Z.S. Wang, Y. Cui, Y. Dan-oh, C. Kasada, A. Shinpo, K. Hara, J. Phys. Chem. C 112 (2008) 17011.
[7] (a) K. Sayama, K. Hara, N. Mori, M. Satsuki, S. Suga, S. Tsukagoshi, Y. Abe, H. Sugihara, H. Arakawa, Chem. Commun. (2000) 1173;
(b) W.J. Wu, J.L. Hua, Y.H. Jin, W.H. Zhan, H. Tian, Photochem. Photobiol. Sci. 7 (2008) 63.
[8] (a) T. Horiuchi, H. Miura, K. Sumioka, S. Uchida, J. Am. Chem. Soc. 126 (2004) 12218;
(b) B. Liu, W.H. Zhu, Q. Zhang, W.J. Wu, M. Xu, Z. Ning, Y. Xie, H. Tian, Chem. Commun. (2009) 1766;
(c) T. Marinado, D.P. Hagberg, M. Hedlund, T. Edvinsson, E.M.J. Johansson, G. Boschloo, H. Rensmo, T. Brinck, L.C. Sun, A. Hagfeldty, Phys. Chem. Chem. Phys. 11 (2009) 133.
[9] K. Hara, T. Sato, R. Katoh, A. Furube, T. Yoshihara, M. Murai, M. Kurashige, S. Ito, A. Shinpo, S. Suga, H. Arakawa, Adv. Funct. Mater. 15 (2005) 246.
[10] (a) Z.S. Wang, F.Y. Li, C.H. Huang, Chem. Commun. (2000) 2063;
(b) Q.H. Yao, F.S. Meng, F.Y. Li, H. Tian, C.H. Huang, J. Mater. Chem. 13 (2003) 1048.
[11] (a) M. Velusamy, K.R.J. Thomas, J.T. Lin, Y.C. Hsu, K.C. Ho, Org. Lett. 7 (2005) 1899;
(b) T. Kitamura, M. Ikeda, K. Shigaki, T. Inoue, N. Anderson, X. Ai, T. Lian, S. Yanagida, Chem. Mater. 16 (2004) 1806;
(c) D.P. Hagberg, T. Edvinsson, T. Marinado, G. Boschloo, A. Hagfeldt, L.C. Sun, Chem. Commun. (2006) 2245;
(d) H.N. Tian, J.X. Pan, R.K. Chen, M. Liu, Q.Y. Zhang, A. Hagfeldt, L.C. Sun, Adv. Funct. Mater. 18 (2008) 3461;
(e) P. Qin, H.J. Zhu, T. Edvinsson, G. Boschloo, A. Hagfeldt, L.C. Sun, J. Am. Chem. Soc. 130 (2008) 8570.
[12] (a) S. Kim, J.K. Lee, S.O. Kang, J. Ko, J.H. Yum, S. Fantacci, F.D. Angelis, D.D. Censo, M.K. Nazeeruddin, M. Grätzel, J. Am. Chem. Soc. 128 (2006) 16701;
(b) D. Kim, J.K. Lee, S.O. Kang, J. Ko, Tetrahedron 63 (2007) 1913;
(c) H. Choi, J.K. Lee, K. Song, S.O. Kang, J. Ko, Tetrahedron 63 (2007) 3115.
[13] (a) C. Zafer, B. Gultekin, C. Ozsoy, C. Tozlu, B. Aydin, S. Icli, Sol. Energy Mater. Sol. Cells 94 (2010) 655;
(b) C. Teng, X.C. Yang, C.Z. Yuan, C.Y. Li, R.K. Chen, H.N. Tian, S.F. Li, A. Hagfeldt, L.C. Sun, Org. Lett. 11 (2009) 5542;
(c) K. Hara, Z.S. Wang, Y. Cui, A. Furube, N. Koumura, Energy Environ. Sci. 2 (2009) 1109;
(d) Z.S. Wang, N. Koumura, Y. Cui, M. Takahashi, H. Sekiguchi, A. Mori, T. Kubo, A. Furube, K. Hara, Chem. Mater. 20 (2008) 3993.
[14] R.Q. Chen, X.C. Yang, H.N. Tian, L.C. Sun, J. Photochem. Photobiol. A 189 (2007) 295.
[15] (a) H.N. Tian, X.C. Yang, R.K. Chen, Y.Z. Pan, L. Li, A. Hagfeldt, L.C. Sun, Chem. Commun. (2007) 3741;
(b) H.N. Tian, X.C. Yang, J.Y. Cong, R.K. Chen, C. Teng, J. Liu, Y. Hao, L. Wang, L.C. Sun, Dyes Pigments 84 (2010) 62;
(c) S.S. Park, Y.S. Won, Y.C. Choi, J.H. Kim, Energy Fuels 23 (2009) 3732;
(d) Z.B. Xie, A. Midya, K.P. Loh, S. Adams, D.J. Blackwood, J. Wang, X.J. Zhang, Z.K. Chen, Prog. Photovolt.: Res. Appl. 18 (2010) 573;
(e) W.J. Wu, J.B. Yang, J.L. Hua, J. Tang, L. Zhang, Y.T. Long, H. Tian, J. Mater. Chem. 20 (2010) 1772.
[16] J. Tang, W.J. Wu, J.L. Hua, J. Li, H. Tian, Energy Environ. Sci. 2 (2009) 982.
[17] D. Liu, R.W. Fessenden, G.L. Hug, P.V. Kamat, J. Phys. Chem. B 101 (1997) 2583.
[18] (a) J. Tang, J.L. Hua, W.J. Wu, J. Li, Z.G. Jin, Y.T. Long, H. Tian, Energy Environ. Sci. 3 (2010) 1736;
(b) Z.J. Ning, Q. Zhang, W.J. Wu, H.C. Pei, B. Liu, H. Tian, J. Org. Chem. 73 (2008) 3791;
(c) C. Teng, X.C. Yang, S.F. Li, M. Cheng, A. Hagfeldt, L.Z. Wu, L.C. Sun, Chem. Eur. J. 16 (2010) 13127;
(d) L. Alibabaei, J.H. Kim, M. Wang, N. Pootrakulchote, J. Teuscher, D. Di Censo, R. Humphry-Baker, J.-E. Moser, Y.-J. Yu, K.-Y. Kay, S.M. Zakeeruddin, M. Grätzel, Energy Environ. Sci. 3 (2010) 1757.
[19] K.R.J. Thomas, Y. Hsu, J.T. Lin, K. Lee, K. Ho, C. Lai, Y. Cheng, P. Chou, Chem. Mater. 20 (2008) 1830.
[20] A. Hagfeldt, M. Grätzel, Chem. Rev. 95 (1995) 49.
[21] M.J. Frisch, G.W. Trucks, H.B. Schlegel, G.E. Scuseria, M.A. Robb, J.R. Cheeseman, J.A. Montgomery Jr., T. Vreven, K.N. Kudin, J.C. Burant, J.M. Millam, S.S. Iyengar, J. Tomasi, V. Barone, B. Mennucci, M. Cossi, G. Scalmani, N. Rega, G.A. Petersson, H. Nakatsuji, M. Hada, M. Ehara, K. Toyota, R. Fukuda, J. Hasegawa, M. Ishida, T. Nakajima, Y. Honda, O. Kitao, H. Nakai, M. Klene, X. Li, J.E. Knox, H.P. Hratchian, J.B. Cross, V. Bakken, C. Adamo, J. Jaramillo, R. Gomperts, R.E. Stratmann, O. Yazyev, A.J. Austin, R. Cammi, C. Pomelli, J.W. Ochterski, P.Y. Ayala, K. Morokuma, G.A. Voth, P. Salvador, J.J. Dannenberg, V.G. Zakrzewski, S. Dapprich, A.D. Daniels, M.C. Strain, O. Farkas, D.K. Malick, A.D. Rabuck, K. Raghavachari, J.B. Foresman, J.V. Ortiz, Q. Cui, A.G. Baboul, S. Clifford, J. Cioslowski, B.B. Stefanov, G. Liu, A. Liashenko, P. Piskorz, I. Komaromi, R.L. Martin, D.J. Fox, T. Keith, M.A. Al-Laham, C.Y. Peng, A. Nanayakkara, M. Challacombe, P.M.W. Gill, B. Johnson, W. Chen, M.W. Wong, C. Gonzalez, J.A. Pople, Gaussian 03, Revision B.05, Gaussian, Inc., Wallingford, CT, 2004.
[22] Z.J. Ning, Y.C. Zhou, Q. Zhang, D.G. Ma, J.J. Zhang, H. Tian, J. Photochem. Photobiol. A: Chem. 192 (2007) 8.
[23] A. Hagfeldt, M. Grätzel, Acc. Chem. Res. 33 (2000) 269.
[24] P. Bonhôte, A.P. Dias, N. Papageorgiou, K. Kalyanasunda-ram, M. Grätzel, Inorg. Chem. 35 (1996) 1168.
[25] J. Liu, H.T. Yang, W.W. Tan, X.W. Zhou, Y. Lin, Electrochim. Acta 56 (2010) 396.
[26] W. Xu, B. Peng, J. Chen, M. Liang, F.S. Cai, J. Phys. Chem. C 112 (2008) 874.
[27] N.B. McKeown, S. Badriya, M. Helliwell, M. Shkunov, J. Mater. Chem. 17 (2007) 2088.